Romanian Reports in Physics, Vol. 66, No. 2, P. 574–592, 2014

ELEMENTARY TIGHT-BINDING METHOD FOR SIMPLE ELECTRONIC STRUCTURE CALCULATIONS – AN EDUCATIONAL APPROACH TO MODELING CONJUGATED DYES FOR DYE-SENSITIZED SOLAR CELLS

ANAMARIA TRANDAFIR, ADRIAN TRANDAFIR, CORNELIU I. OPREA, MIHAI A. GÎRȚU

[1] "Ovidius" University of Constanța, Department of Physics, Constanța 900527, Romania,
E-mail: mihai.girtu@univ-ovidius.ro

Received January 15, 2014

Abstract. Based on the experience gained during an introductory course in physics of materials, we argue that the tight-binding method, in its simplest form, is a useful tool for understanding the properties of finite molecular systems. We illustrate the applicability of this approach to study the electronic spectrum of several coumarin-based dyes successfully used in fabricating dye-sensitized solar cells. We show how the students can find the energy levels and the corresponding molecular orbitals of the dyes as well as how they can explain experimental results demonstrating the red-shift of the absorption spectrum and the improved charge injection.

Key words: physics education, physics of materials, tight binding approximation, electronic spectrum, band-gap engineering, conjugated dyes, dye-sensitized solar cells.

1. INTRODUCTION

The electronic structure of molecules and solids is a topic of interest in most physics curricula. Whether offered in the general modern physics or solid state physics classes or in more specialized materials physics courses, the notions of electronic energy states and orbitals are key to the understanding of some basic physical properties and phenomena.

A well known approach of describing electronic states in a crystalline solid is based on the tight-binding approximation, which constructs the wave functions of the system as superpositions of wave functions of electrons strongly localized on each atomic site. The method is based on writing the molecular orbitals as linear combinations of atomic orbitals (LCAO), approach widely used in chemistry. In fact, the LCAO method for molecules was introduced in chemistry in 1928 by Finklestein and Horowitz [1], while the corresponding LCAO method for solids was developed by Bloch at about the same time [2].

The typical tight-binding method makes further use of Bloch's theorem, which imposes constraints on the wave functions based on the periodicity of the lattice [3, 4]. An alternative approach to taking into account the periodicity is to build the solid from atoms or molecules and to describe the bands starting from the chemistry concept of bonds [5, 6]. The simplest method used in chemistry textbooks is the Hückel molecular orbital theory [7], which corresponds well to the tight-binding approach, employed for describing extended solid state systems. The Hückel method has been widely used in chemistry courses due to its simplicity, which makes it an excellent pedagogical tool for introducing some abstract notions, particularly the electron densities and the orbital energies, but also for illustrating concepts such as molecular symmetry and orbital topology [8]. For these reasons, the use of the Hückel approach has been extensively covered in chemical education journals [9–18]. In contrast, the tight-binding approach has not received the attention it deserves in physics education journals, one of the few meaningful examples being the calculation of densities of states in solid state physics [19]. In that paper, the authors stress that: 'Students can gain much insight into solid state research from this method since it helps to bridge the gap between the standard textbook treatments and the highly technical discussions of the research literature.' [19].

Inspired by such motivating statements, we attempted to use these concepts and methods in teaching a college level introductory course in the physics of materials. We think that addressing this topic is timely also in Romania, as although the interest in physics education is high both at secondary and tertiary levels, most of the publications deal with improving teaching of physics in high-schools. It is worth mentioning that, of the papers focusing on physics education, some concentrate on using computer assisted methods [20, 21] and others on making topics in photovolatics more familiar to students [22–24]. Our work complements these approaches, as it attempts to demonstrate that the simple tight-binding method, together with some basic computer algebra software, can significantly improve the understanding of college level materials physics concepts. One expected learning outcome of that class is that the students acquire the basic knowledge regarding the electronic and photonic properties of molecular systems, as well as some basics on organic electronics with applications in organic optoelectronic devices.

Based on the experience gained in teaching that class, we argue in this paper that the tight-binding method, in its simplest form, corresponding to the Hückel approach, can be a simple and useful tool for understanding the properties of some finite molecular systems. The method has already been used to find the crystal orbitals for one-dimensional chains of *p* orbitals [4] or, equivalently, for linear conjugated polymers, such as polyacetylene [8]. Here however, we illustrate our ideas by applying the tight-binding (TB) approach to various coumarin-based dyes successfully used in fabricating dye-sensitized solar cells (DSSC) [25, 26].

The method can be easily applied to conjugated organic systems, such as some of the dyes used in DSSCs [27] or in organic light emitting devices [28, 29]. DSSCs are low cost photovoltaic devices in which light is absorbed into a dye attached to a wide bandgap semiconductor such as TiO_2. The excited electron is transfered from the dye to the oxide nanoparticles, diffuses through the porous film to the photoanode, does work in the external circuit and is brought back from the counter-electrode to the dye by either a redox electrolyte or an organic hole transporter. High photovoltaic conversion efficiencies have been obtained for DSSCs initially with ruthenium(II)-based dyes and a iodide-triiodide electrolyte (over 11%) [26] and, more recently, with zinc(II)-porphyrin dyes with a cobalt complex as a liquid electrolyte (over 12%) [30]. Even more recently, a record efficiency of 15% has been reached with perovskite nanoparticles as TiO_2 sensitizers and a solid organic hole transporter [31].

The conversion efficiencies of metal-free organic dyes are lower (less than 10%), but they display other features, such as lower costs, tunable bandgaps by small variations of the molecular structure, which typically consists of a π-conjugated donor-acceptor system [32]. Among the metal-free organic dyes used in DSSCs, coumarin-based ones have shown good photoresponse in the visible region, long-term stability under light exposure, appropriate energy level alignment for injection into the conduction band of TiO_2 [33, 34]. The molecular structures of various coumarin-based dyes are shown in Fig. 1.

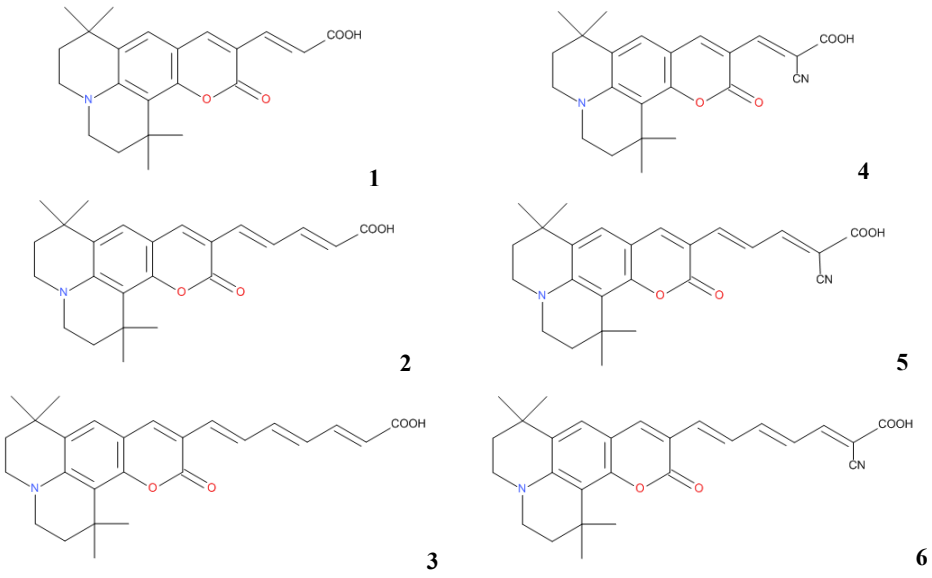

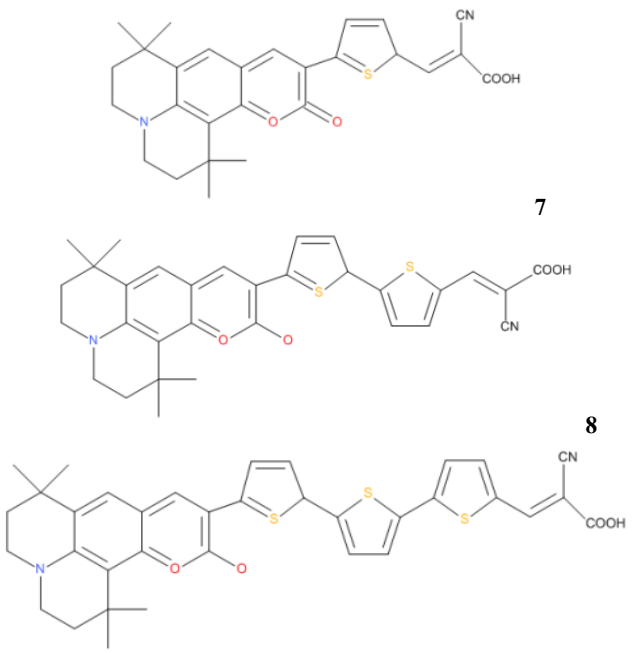

Fig. 1 – Schematic molecular structures of some coumarin-based dyes [36, 37]: **1** = NKX-2398, **4** = NKX-2388, **5** = NKX-2311, **6** = NKX-2586, **7** = NKX-2587, **8** = NKX-2677, **9** = NKX-2697.

Initially, devices with a photovoltaic conversion efficiency of 5.6% were reported using a dye named NKX-2311 (structure **5** in Fig. 1) [35, 36]. Later on, the NKX-2677 dye (structure **8** in Fig. 1) has been used successfully as a photosensitizer in DSSCs with an even larger efficiency of up to 7.4% [37]. The stability under sun soaking and the efficiency were further improved, reaching 8.2% with NKX-2700 [38], by means of a thiophene-based bridge between the donor/acceptor parts of the molecule. Various other coumarin-based dyes have been synthesized and studied as TiO_2 sensitizers [32, 34].

Here, for a more systematic study, we apply the simple TB approach to nine coumarin-based dyes which differ by the number of ethenyl (vinyl) groups and by the presence of cyano and thiophene groups. We illustrate the role of the ethenyl and thiophene groups on fine tunning the gap between the ground and excited states and the influence of the cyano group on the overall charge distribution. We discuss intuitively the likelihood of the charge transfer from the dye to the TiO_2 substrate illustrating concepts that are accessible at the level of junior and senior physics students. Exploiting numerical functions of algebraic software, which provide the eigenvalues and eigenvectors of the energy matrix, we can provide a qualitative discussion of the influence of various dye constituents on the electronic spectra, exemplifying the power of the simple TB method in explaining the

properties of such materials. In the end, only to specify more clearly the limits of this simple approach we compare its results with the ones provided by a widely used quantum chemistry package.

2. TIGHT-BINDING APPROACH TO CONJUGATED SYSTEMS

The TB method has as prerequisites some simplifying approximations made because of the difficulty in solving the many-body Schrödinger equation for all the electrons and nuclei in the solid. A first approximation is that the nuclei are frozen in their lattice positions, such that we can treat the electrons separately. Next we assume that the electrons can be described by a single electron problem, in which they feel only the mean field of the other ions and electrons [3, 4].

The basic assumption of the tight-binding approximation is that we can use the wavefunctions of electrons tightly bound to the atoms as a basis for expanding the crystal or molecular wavefunctions. As we deal here with finite molecular systems we assume that the molecular orbitals can be written as a linear combination of atomic orbitals:

$$\psi_{m,i}(\mathbf{r}) = \sum_{m',i'} c_{m,i;m',i'} \phi_{m'}(\mathbf{r} - \mathbf{r}_{i'}), \tag{1}$$

where $\phi_m(\mathbf{r} - \mathbf{r}_i)$ is an atomic orbital of the electron bound to the i-th nucleus.

We can construct matrix elements of the single-particle Hamiltonian, H, between the various atomic orbitals [4]:

$$H_{m,i;m',i'} = \langle \phi_m(\mathbf{r} - \mathbf{r}_i) \,|\, H \,|\, \phi_{m'}(\mathbf{r} - \mathbf{r}_{i'}) \rangle, \tag{2}$$

the number of rows and columns being equal to the number of atomic orbitals considered. Also, the overlap integrals are

$$S_{m,i;m',i'} = \langle \phi_m(\mathbf{r} - \mathbf{r}_i) \,|\, \phi_{m'}(\mathbf{r} - \mathbf{r}_{i'}) \rangle. \tag{3}$$

The TB approach makes use of the variational principle to determine the energy and the LCAO coefficients of the crystal or molecular wavefunctions. The variational principle leads to a set of equations that can be written in a matrix form, involving the energy matrix as well as the column of the LCAO coefficients from Eq. (1):

$$\begin{pmatrix} H_{11} - ES_{11} & H_{12} - ES_{12} & \dots & H_{1n} - ES_{1n} \\ H_{21} - ES_{21} & H_{22} - ES_{22} & \dots & H_{2n} - ES_{2n} \\ \vdots & \vdots & \vdots & \vdots \\ H_{n1} - ES_{n1} & H_{n2} - ES_{n2} & \dots & H_{nn} - ES_{nn} \end{pmatrix} \cdot \begin{pmatrix} c_1 \\ c_2 \\ \vdots \\ c_n \end{pmatrix} = 0 \tag{4}$$

The roots of the secular determinant are the energies of the molecular orbitals. They can be further used in the matrix equation (Eq. (4)) to determine the LCAO coefficients.

We further make some more simplifying assumptions. First, we concentrate on the valence electrons, keeping in mind that the other electron energies lie much lower in the spectrum. For the case of interest here, where we deal with conjugated organic molecules, this approximation means that we can concentrate on the *p* orbitals, neglecting the contribution of the inner electrons. Therefore we can index the orbitals only by the number of the atom it primarily belongs to: $\phi(\mathbf{r}-\mathbf{r}_i)$.

The electron being strongly bound to the nucleus of the atom to which it belongs, we assume that the diagonal matrix elements consist of the energy, ε, of the electron located in the $\phi(\mathbf{r}-\mathbf{r}_i)$ atomic orbital. The energy ε is negative, as we deal with a bound state. Furthermore, we presuppose that the electron can also hop back and forth only between nearest neighbors. The hopping (transfer) integral, *t*, is then nonzero only between adjacent atoms. These approximations can be written [4]:

$$H_{ij}=\begin{cases}\varepsilon, \text{ if } i=j,\\ t, \text{ if } i\neq j, \text{ but adjacent atoms}\\ 0, \text{ all other cases.}\end{cases} \tag{5}$$

Moreover, we consider the orbitals almost orthogonal (very weak overlap):

$$S_{ij}=\delta_{ij}. \tag{6}$$

We have now set the ground for the use of this simple TB approach to several coumarin-based dyes used in DSSCs.

3. RESULTS AND DISCUSSION

The present section is structured in five subsections. The first exposes in some detail the method and all the procedures followed by the students, applied to a very simple example, the basic coumarin. The next three subsections illustrate the power of this elementary approach to reveal the role of various dye constituents (such as the ethenyl, cyano, and thiophene groups) on the electronic structure and optical properties of the dyes. The last subsection clarifies the limits of the simple TB method.

3.1. ILLUSTRATION OF THE METHOD ON THE BASIC COUMARIN

The students start by analyzing the structure of the conjugates system, labeling the atoms and counting the number of $2p_z$ electrons. In the case of the dyes

of interest here the atoms with crucial contributions to the electronic properties of the dyes are mainly carbon, nitrogen, oxygen and sulfur.

The key parameters are the energy of the $2p_z$ orbital, ε and the hopping integral, t, between two carbon atoms, as mentioned above. The corresponding parameters for the other atoms are: $\varepsilon_{O'◆◆} = \varepsilon + 2t$ and $t_{C-O'◆◆} = 0.8t$ and $\varepsilon_{O''} = \varepsilon + t$ and $t_{C=O''} = t$, for oxygen atoms involved in single or double bonds, respectively [8]. The nitrogen atom bound to three carbon atoms is characterized by: $\varepsilon_N = \varepsilon + 1.5t$ and $t_{C-N} = 0.8t$, whereas for the S atom we have: $\varepsilon_S = \varepsilon$ and $t_{C-S} = 0.8t$ [8, 39]. We illustrate the method described above by applying it to the basic coumarin, shown in Fig. 2.

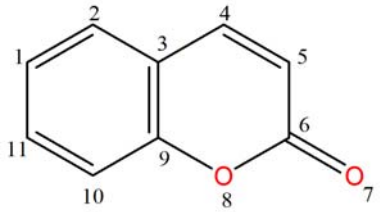

Fig. 2 – Schematic molecular structure of the basic coumarin showing the atom numbering.

Taking into account one $2p_z$ orbital per atom, the students construct by linear combinations, eleven molecular orbitals. Of the eleven atoms, nine are carbon, the other two are oxygen atoms, one with two single bonds and the other with a double bond. Next, they build the energy matrix. The result is a 11×11 matrix, which has nonzero terms on the main diagonal (the energy of the electron in its own atomic orbital) and next to it (the terms describing the transfer to the nearest neighbors on both sides:

$$\begin{pmatrix} \varepsilon - E & t & 0 & 0 & 0 & 0 & 0 & 0 & 0 & 0 & t \\ t & \varepsilon - E & t & 0 & 0 & 0 & 0 & 0 & 0 & 0 & 0 \\ 0 & t & \varepsilon - E & t & 0 & 0 & 0 & 0 & 0 & 0 & 0 \\ 0 & 0 & t & \varepsilon - E & t & 0 & 0 & 0 & 0 & 0 & 0 \\ 0 & 0 & 0 & t & \varepsilon - E & t & 0 & 0 & 0 & 0 & 0 \\ 0 & 0 & 0 & 0 & t & \varepsilon - E & t'' & t' & 0 & 0 & 0 \\ 0 & 0 & 0 & 0 & 0 & t'' & \varepsilon_{O''} - E & 0 & 0 & 0 & 0 \\ 0 & 0 & 0 & 0 & 0 & t' & 0 & \varepsilon_{O'} - E & t' & 0 & 0 \\ 0 & 0 & 0 & 0 & 0 & 0 & 0 & t' & \varepsilon - E & t & 0 \\ 0 & 0 & 0 & 0 & 0 & 0 & 0 & 0 & t & \varepsilon - E & t \\ t & 0 & 0 & 0 & 0 & 0 & 0 & 0 & 0 & t & \varepsilon - E \end{pmatrix} \cdot \begin{pmatrix} c_1 \\ c_2 \\ c_3 \\ c_4 \\ c_5 \\ c_6 \\ c_7 \\ c_8 \\ c_9 \\ c_{10} \\ c_{11} \end{pmatrix} = 0, \quad (7)$$

E is the energy of the molecular orbital. With a change of variable, $x = (\varepsilon - E)/t$, the matrix is further simplified, with only x, 1 and 0 elements. Thus, the energy is expressed in units of t.

The next step is to solve the secular equation, setting to zero the determinant of the matrix. The roots of the secular equation provide the energy values of the molecular orbitals. They are further used to determine from the matrix equation the coefficients of the atomic orbitals in the expansion of the corresponding molecular orbitals.

Numerical functions of algebraic computer programs such as Mathematica [40], MathCAD [41], Maple [42], etc., can solve the secular determinant and the matrix equation, as already shown [13, 16]. The actual commands used by our students to determine the eigenvalues and the corresponding eigenvectors of the energy matrix are displayed in the supplementary materials [43].

Along with the counting of the $2p_z$ orbitals the students need to count the valence electrons, the electrons that can delocalize in molecular orbitals with π character. If in the case of carbon atoms with sp^2 hybridization the counting is easy, one $2p_z$ electron per atom, for nitrogen, oxygen or sulfur the number of electrons involved depends on the type of bonding between the heteroatom and the neighboring carbon atoms [8, 10, 12, 39]. For instance, the atom O8 has two electrons involved in the σ bonds to C6 and C9 and other two in a lone pair; therefore, two electrons are left to contribute to the $2p_z$ orbital. In contrast, O7 has one electron involved in a σ bond to C6 and four electrons in two lone pairs; hence only one electron is left in a $2p_z$ orbital to participate in π bonding. Consequently, coumarin has 11 orbitals and 12 electrons.

The results of the calculations are shown in Fig. 3, which displays the energy diagram [14] with the valence energy levels of the basic coumarin dye. The eleven MOs are occupied by the 12 electrons following Pauli's principle, with at most two electrons starting from the one of the lowest energy. Therefore, the first six orbitals are doubly occupied and the rest are empty. The highest occupied (HO) MO lies just below the energy origin (taken as the energy of the $2p_z$ orbital of carbon), whereas the lowest unoccupied (LU) MO is located just above the origin.

The optical properties of the dye are dictated to a large extent by the HOMO to LUMO transition. Particularly, the absorption wavelength is determined by the energy difference between the two orbitals: $\Delta E = E_{\mathrm{LUMO}} - E_{\mathrm{HOMO}}$. The wavelength of the main optical transitions in the case of the basic coumarin dye can be determined from the relation $hc/\lambda = \Delta E = 0.886t$.

The values of the TB parameters have been fitted based on various experimental data sets [8]. A typical set, obtained from the consideration of experimental heats of atomization, is $\varepsilon = -11.26030$ eV [44], and $t = -1.4199$ eV [45]. Correspondingly, the wavelength would be $\lambda \approx 986$ nm, in the near infrared, which is a poor approximation, as coumarin is transparent and the main optical transition extends in the ultraviolet, not the infrared. As we shall see in later

sections, the TB approach cannot render quantitatively exact gaps but it describes qualitatively correct many electro-optical properties.

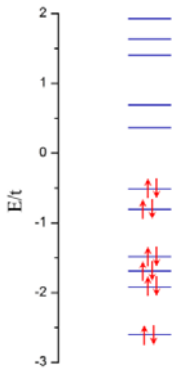

Fig. 3 – Schematic representation of the energy spectrum of the basic coumarin dye. Six of the eleven MOs are occupied by the 12 electrons. The origin of the axis is at ε, the energy of the $2p_z$ level of carbon, and the scale is expressed in units of t.

Some of the MOs are displayed in Fig. 4, using a simple widely available visualisation program [46]. The diagram is a schematic top view of the MOs with π symmetry. The sizes and colors of the discs are correlated with the magnitude and sign of the coefficient of the AO in the MO expansion [18].

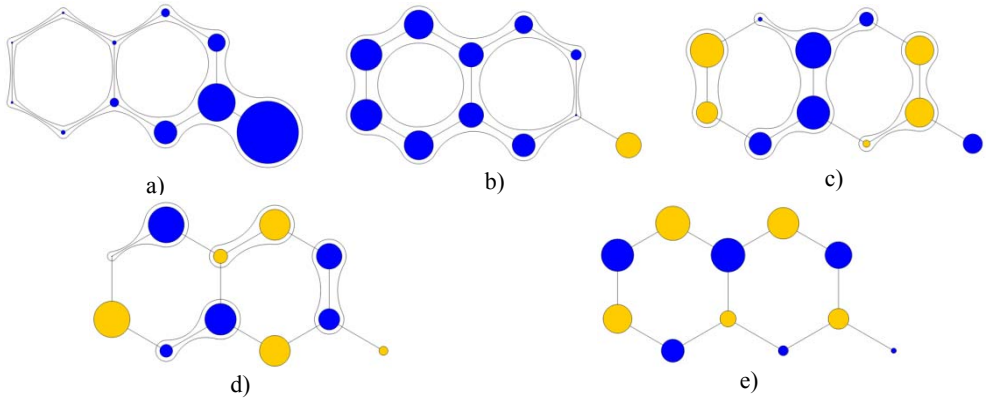

Fig. 4 – Schematic representation of some molecular orbitals of the basic coumarin dye: a) first MO (of lowest energy); b) second MO; c) HOMO; c) LUMO; d) eleventh MO (of highest energy).

For the orbital with the lowest energy all coefficients have the same sign, resulting in no transverse nodal planes. The electron is delocalized over the entire molecule but the charge is mainly distributed on and around the oxygen atom with the double bond (atom number 7 in Fig. 2). The second state has one transverse

nodal plane and the eleventh state has the maximum number of nodal planes, the sign of the coefficients changing from one atom to the next. Looking in between, at the key MOs, the LUMO has one extra nodal plane than the HOMO.

Thus, the students can visualize the charge distribution in the dye and correlate the increase in the kinetic energy with the increase in the number of transverse nodal planes of the corresponding MO.

3.2. ROLE OF THE ETHENYL GROUPS

In the attempt to increase the photovoltaic conversion efficiency of the DSSCs one of the key requirements is a better matching of the absorption spectrum of the dye with the solar irradiation spectrum [27]. It was shown experimentally [36] that the spectra of organic dyes which absorb in the UV can be red-shifted by expansion of the π conjugation, *i.e.* by insertion of ethenyl groups in the dye backbone.

In this section we study the effect of the ethenyl groups on the optical spectra of the dyes. To better understand the origin of the red-shift of the optical spectra, the students can perform a systematic comparative analysis of the spectra of dyes **1**, **2** and **3**, as well as **4**, **5**, and **6**, as they differ by an increasing number of ethenyl groups (Fig. 1).

Following the procedure already illustrated in the previous section the students start from the minimal number of atomic orbitals participants in charge conjugation [10, 12]. Referring to dye **1**, we have 17 $2p_z$ AOs, one for each atom. In addition to the 12 $2p_z$ electrons from the basic coumarin, we have 3 from the extra C atoms, 3 from the O atoms of the carboxyl group (one for =O and two for –O–) and 2 from the N atom, resulting in 20 electrons. Additionally, each ethenyl as well as each cyano group participates with 2 electrons. Therefore, the numbers of orbitals are 17, 19, 21, and 19, 21, 23 for dyes **1**, **2**, **3**, and **4**, **5**, **6**, respectively. In each of these cases the number of electrons exceeds by three the number of orbitals.

The energy of the key orbitals involved in the main optical transition is shown as a function of the number of ethenyl units in Fig. 5. Dyes **1** and **4**, have only one ethenyl unit, **2** and **5**, have two whereas **3** and **6**, three. It can be seen that an increased number of ethenyl groups systematically lowers the LUMO and increases the HOMO such that, overall, there is a decrease of ΔE, which shifts the optical spectrum to higher wavelengths. This redshift of the wavelength with longer conjugated bridges is clearly seen in Fig. 5b.

To better understand these trends, the students can draw the key MOs, as displayed in Fig. 6. They first note that the charge distributions in the MOs of the coumarin-based dyes correspond well to those of the basic coumarin, shown in Fig. 4c and 4d.

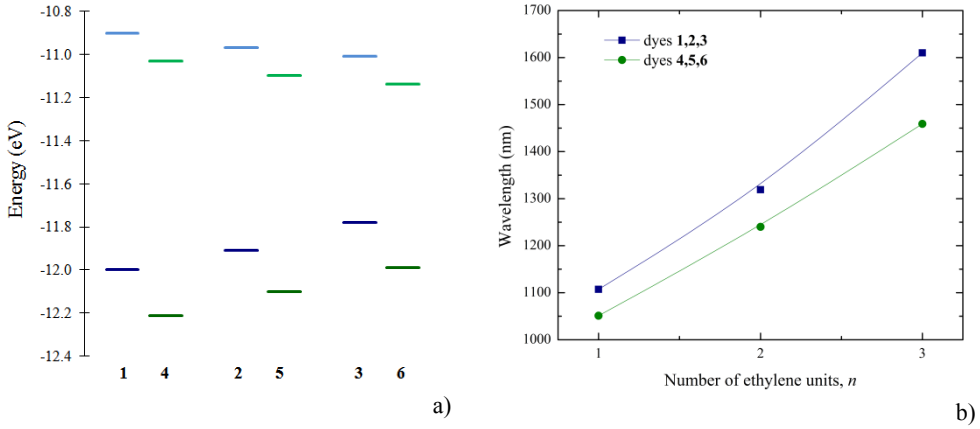

Fig. 5 – Gap between the LUMOs (higher levels) and HOMOs (lower levels) of the coumarin-based dyes, a), and the wavelength of the optical transition, b), as functions of the number of ethenyl groups. Dyes **4**, **5**, **6** differ from dyes **1**, **2**, **3**, respectively, only by the additional cyano group.

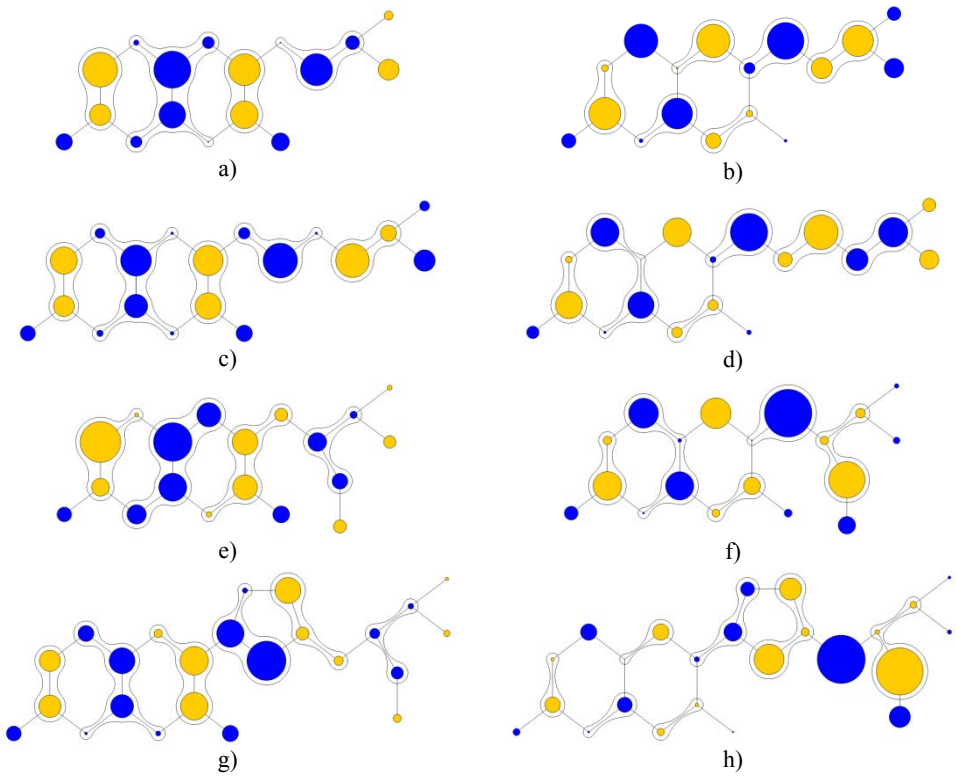

Fig. 6 – Schematic representation of the key molecular orbitals of some coumarin-based dyes: a) HOMO; b) LUMO of **1**; c) HOMO; d) LUMO of **2**; e) HOMO; f) LUMO of **4**; g) HOMO; h) LUMO of **7**.

Comparing the HOMOs of dyes **1** and **2** (Fig. 6a and 6c) we note that there is one more transverse nodal plane due to the presence of the additional ethenyl group, which leads to a slight increase in energy, as seen in Fig. 5. In contrast, in the case of the LUMO, the charge is redistributed on dye **2**, the additional bonds on the rings lowering the energy.

The students can easily understand these results also by analogy with the problem of the particle in the one-dimensional potential well. Just as in the case of the electron in a box, the increased width of the well leads to an overall lowering of the energy for each state as well as a decrease in the spacing between consecutive energy levels [10, 12, 14]. Here, the lengthening of the conjugated bridge of the dye extends the distance within which the movement of the electron is confined, leading to smaller differences between the energy levels.

A more thorough analysis of the band gap engineering in π-conjugated systems takes into account the effects of 'bond length alternation' and of *aromatic stabilization* [47]. It was found experimentally that the gap increases with the bond length alternation (with the difference between the length of the single and the double bonds) and with the decrease of the number of carbon atoms along the conjugated chain [47, 48]. Also, the π-electrons tend to be confined on the aromatic ring leading to wider gaps and transitions in the UV. Hence, for better matching of the absorption spectrum of the dyes with the solar spectrum, it is desirable to lower the gap by insertion of double bonds, which cause a charge delocalization along the whole conjugated system, taking away some of the charge from the aromatic rings [14, 47]. Although the simple TB method does not take into account any variations in the bond length, overall, these experimental observations can easily be understood by the students based on the simple calculations described above.

3.3. ROLE OF THE CYANO GROUPS

The dyes used in DSSCs have D–π–A structure, possessing both electron-donating (D) and electron-accepting (A) groups, linked by π–conjugated bridges. For the dyes of interest here, the electron-donating part can be associated with the coumarin and the electron-accepting unit with the carboxyl group. Such a structure illustrates the *Push*$\rightarrow$*Pull* concept [27, 34]: due to light absorption during the HOMO$\rightarrow$LUMO transition, the charge density moves from the donor group to the acceptor group, getting closer to the TiO_2 substrate. Experimentally, it was shown [36] that due to its strong electron-withdrawing abilities, the cyano group connected to the anchoring carboxyl enhances the 'Push$\rightarrow$Pull' effect. Consequently, the –C≡N group plays an important role in the effective electron injection into the conduction band of the semiconducting oxide.

To explain these experimental observations the students can compare the dyes already studied, this time in pairs: **1** and **4**, **2** and **5**, and **3** and **6**. As mentioned above, the extra cyano group brings two additional electrons in the calculations. We return to Fig. 5, which displays the pairs of dyes with the same number of

ethenyl groups but differing by the additional cyano group. We note that the presence of the –C ≡ N group systematically causes a general shift towards lower energies of both HOMOs and LUMOs, for all the three pairs of dyes. The shift is stronger for the HOMOs, with an average of 0.19 eV, compared to the 0.13 eV for the LUMOs. Consequently, the gap is larger for the dyes with cyano groups.

To understand intuitively these results, the students can analyze the MOs drawn schematically in Fig. 6. Comparing the MOs of dyes **1** and **4** one notes the bond between the carbon atoms of the dye backbone and of the cyano group, which lowers the energy. Thus, both the HOMO and the LUMO of dye **4** lie lower than the corresponding orbitals of **1**.

Furthermore, looking at the HOMOs of Figs. 6a and 6d, it can be seen that the –C ≡ N group tends to keep the charge density distributed more on the coumarin side of the dye. In contrast, the LUMOs (Fig. 6b and 6f) have less charge on the coumarin and more on the π-bridge and on the carbon atom of the cyano group. Due to the stronger Coulomb attraction of the electron to the nitrogen nucleus and to the presence of the triple bond, –C ≡ N acts as an electron withdrawing group. This is a clear illustration of an increased *Push*→*Pull* effect by small alterations of the conjugated backbone near the anchoring carboxyl group of the dye.

3.4. ROLE OF THE THIOPHENE GROUPS

The dye elongation with ethenyl groups discussed above contributes to a red shift in the absorption spectrum. However, it can also decrease the stability of the dye molecule, due to the possibility of isomer formation. It was demonstrated experimentally [37] that the introduction of π-conjugated ring moieties such as thiophene, into the dye backbone expands the π-conjugation system, improving in the same time the stability of the molecule.

To explain these experimental results the students can explore the role of the number of thiophene rings on the energy spectrum of the dyes. For that purpose, we compare dyes **7**, **8** and **9**. The calculations lead to the key energy levels displayed in Fig. 7.

We first note that the energy gaps between the LUMOs and the HOMOs are significantly smaller for the dyes with thiophene rings compared to the ones with simple backbones. Consequently, the wavelengths of the optical transitions displayed in Fig. 7b are systematically red-shifted with respect to the ones of the dyes **1** to **6** reported in Fig. 5b. The smaller gaps are due mostly to the higher HOMOs, all shifted up likely because of the higher number of transverse nodal planes. The energies of the LUMOs do not differ much because the additional nodal planes seem to be compensated by the stronger charge confinement on the thiophene rings.

Second, here again, it is observed that the energy gap is lowered by a longer π-conjugated system [47]. Consequently, the spectrum is red-shifted for the dyes with more thiophene units.

Third, we notice another illustration of the *Push→Pull* effect, as on the HOMO the charge is delocalized with an important contribution on the coumarin part, whereas on the LUMO the electron is localized towards the opposite side of the dye, next to the anchoring group. Both orbitals show a high electron density on the sulfur atom, as expected for a more electronegative atom.

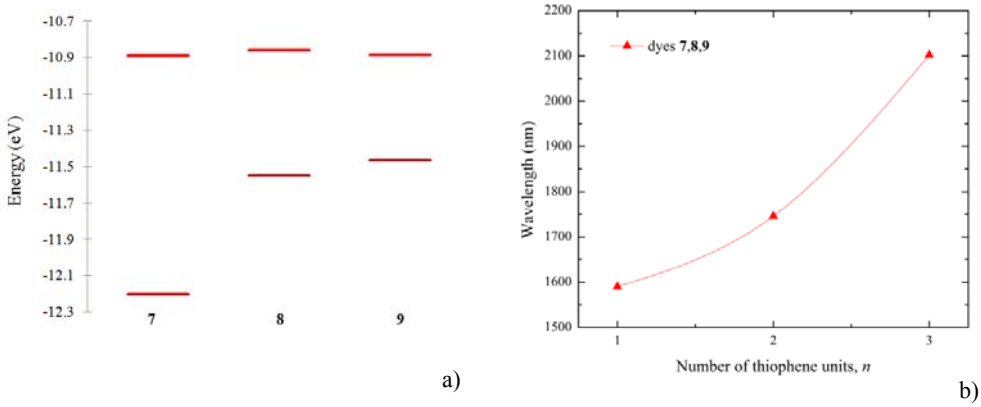

Fig. 7 – Gap between the LUMOs (higher levels) and HOMOs (lower levels) of the coumarin-based dyes with thiophene groups (a), and the wavelength of the optical transition (b), as functions of the number of thiophene groups.

3.5. LIMITS OF THE TIGHT-BINDING APPROACH

Using a simple tight-binding approach we determined qualitatively the energy levels and the corresponding molecular orbitals of nine coumarin-based dyes. The calculations explain well the general experimental trends, particularly the effect of the longer conjugated bridge, as well as the roles of the cyano or thiophene groups. However, to illustrate the quantitative limits of this approach it may be useful to resort to another approach. Although such calculations may be beyond the level of an introductory course in the physics of materials and are not usually performed by the students, we report the results below for proper benchmarking.

Taking as reference the simplest TB approach, the next method, in terms of simplicity, for the calculation of the electronic energies and molecular orbitals is the Extended Hückel (EH) Method [49], which takes into account all valence electrons of all atoms. The hydrogen atoms, which are disregarded in the simple Hückel method, are also taken into account in the extended Hückel calculation. Also, the orbitals are no longer assumed to be orthogonal, the calculations providing an overlap matrix that has many elements different from zero. The energy matrix has as diagonal elements the energy of the electron in the particular atomic orbital of the isolated atom. The nondiagonal elements are determined taking into account the diagonal energies and the corresponding orbital overlaps [8].

The extended Hückel method is not very successful in determining the structural geometry of a molecule but it allows a more accurate computation of the molecular orbitals and their energies. It can also determine the relative energy of different geometrical configurations. It involves calculations in the single-electron approximation and the electron-electron interactions are not explicitly included. Given such limitations the EH method is in itself a crude approximation, as it does not calculate explicitly the energy matrix elements, using parameters fitted from experimental data instead [8]. *Ab initio* calculations are more accurate but are typically beyond the scope of an introduction to the physics of materials and much better suited for a quantum chemistry class. We chose the EH method mainly for its simplicity and particularly to visualize more easily the molecular orbitals.

We performed EH calculations using a commercially available molecular modeling software [50]. The results of the EH calculations are shown in Table 1 and Fig. 8, which display the energies and the electron density of the key states [51], respectively.

We note that the gaps provided by the EH method are larger, in better agreement with the experimental observations [35–38]. Although even the EH method leads to gaps that are smaller than the experimentally observed values, the agreement is clearly better than for the simplest TB approach. Experimentally, the dyes with short conjugated bridges have transitions in the UV limit of the visible range, the spectrum being red-shifted for longer π–conjugation paths. The differences between the results of the two approaches show that the experimental parameters used in the TB scheme, particularly the value of the transfer integral, t, is too small. Also, looking at the sets of dyes, the largest differences between the EH and the TB results are found for the thiophene-based dyes. In those cases, the TB transfer parameter for the sulfur-carbon hopping was even lower, leading to smaller gaps.

Table 1

Energies of the key MOs of coumarin-based dyes calculated by TB and EH methods, expressed in eV

Dye	**1**	**2**	**3**	**4**	**5**	**6**	**7**	**8**	**9**
TB									
E_{LUMO}	-10.87	-10.94	-10.97	-10.99	-11.06	-11.10	-10.89	-10.86	-10.89
E_{HOMO}	-11.98	-11.87	-11.74	-12.17	-12.07	-11.96	-11.67	-11.55	-11.46
ΔE	1.12	0.94	0.77	1.18	1.01	0.86	0.78	0.69	0.58
EH									
E_{LUMO}	-9.79	-9.93	-10.01	-9.87	-10.04	-10.14	-9.79	-9.76	-9.79
E_{HOMO}	-11.5	-11.48	-11.42	-11.5	-11.48	-11.45	-11.23	-11.15	-11.10
ΔE	1.71	1.55	1.41	1.63	1.43	1.30	1.44	1.38	1.30

Examining the differences between the three sets of dyes we observe that the gap calculated by the EH approach decreases with the length of the π–conjugated bridge, consistent with the TB results and the experimental observations [47].

If we compare the actual values of the gaps of pairs of dyes (**4** and **1**, **5** and **2**, **6** and **3**) we note that in EH the presence of the cyano group does not increase the gap, on the contrary. Also, as already mentioned, in EH the presence of the tyophene groups does not decrease as much the gap.

Analyzing the electron densities of the MOs displayed in Fig. 8 in contrast with the schemes exposed in Fig. 6 we note that the EH method indicates the presence of some small electron density also on the saturated rings linked to the coumarin. In the simple TB calculation those atoms were ignored and had no contribution to the charge density.

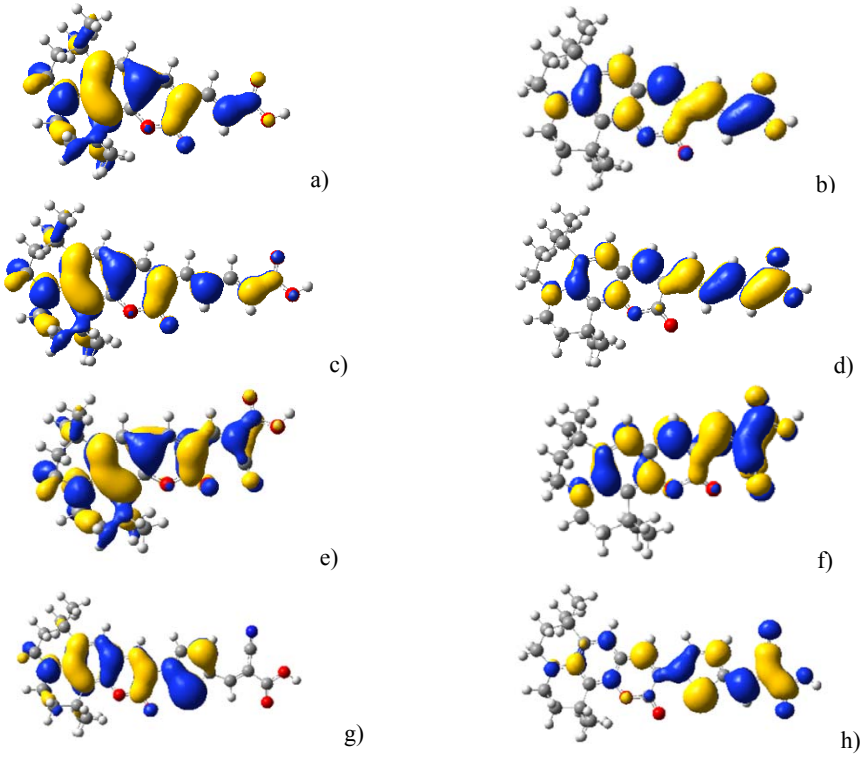

Fig. 8 – Electron density of the key molecular orbitals of some coumarin-based dyes: a) HOMO; b) LUMO of **1**; c) HOMO; d) LUMO of **2**; e) HOMO; f) LUMO of **4**; g) HOMO; h) LUMO of **7**.

Moreover, examining the differences between the HOMOs and the LUMOs we consistently see the *Push*→*Pull* effect for all dyes. Although the charge is delocalized, we can still clearly observe for the HOMOs a sizeable electron density on the rings linked to the coumarin whereas for the LUMOs the charge moves

towards the anchoring carboxyl group. This tendency is important in the DSSCs, where the electron transfer from the excited state of the dye to the TiO_2 substrate is crucial.

Further, looking at dyes **1** and **2** we note that for longer conjugated chains the charge is spread over larger volumes, consistent with our TB results. When comparing dyes **1** and **4** we observe that the presence of additional cyano groups increases the charge density on the anchoring group, facilitating the electron transfer.

Also, examining Figs. 6f and 8f, we find that both approaches indicate a large electron density on the carbon atom between the coumarin and the cyano group. Similarly, the comparison of Figs. 6h and 8h shows a high charge density on the tyophene, particularly on the sulfur atom, consistent in both TB and EH methods.

4. CONCLUSIONS

Encouraged by the use of the simplest form of the tight-binding method to describe extended linear systems with *s* and *p* orbitals [4] as well as by the experience gained over a few years of teaching a senior year introductory course in the physics of materials, we set as a goal to prove that the TB approach can be a useful tool for understanding the properties of some finite molecular systems. We illustrated the applicability of this approach by studying the electronic spectrum of nine coumarin-based dyes which have been successfully used in the fabrication of dye-sensitized solar cells. We presented the steps followed by the students, starting from the analysis of the structure of the conjugated system, the labeling of the relevant atoms, building of the energy matrix, solving the matrix equation, finding the energy levels and the corresponding molecular orbitals, drawing the energy diagrams and the simplest schemes of the molecular orbitals, etc.

To prove the power of this simplest TB approach to qualitatively predict some of the basic optical properties of materials of practical interest we made some systematic comparisons of results obtained for dyes with various lengths of the π–conjugates bridge, as well as with various added constituents, such as cyano and thiophene groups. We were able to explain experimental results demonstrating the red-shift of the absorption spectrum with the increased length of the conjugated backbone when intercalating additional ethenyl groups. We also justified the improved charge injection from the dye to the TiO_2 substrate when cyano groups are added close to the anchoring carboxyl group. Moreover, we analyzed the role of the sulfur atoms closing tyophene rings in increasing the stability of the dyes and in lowering the gap. In summary, with the simplest possible method we could make the basic notions of band gap engineering in molecular systems [47] more easily understandable to our senior physics students.

Finally, we also used more advanced molecular modeling software to clarify the limits of the simple approach proposed. We showed that while experimentally the absorption spectra of the dyes have strong transitions starting from the UV limit

of the spectrum and going to higher wavelengths, the EH method provides transitions in the red limit whereas the simplest TB approach leads to lines in the IR. Therefore, although not accurate enough EH clearly improves over the simplest TB, a better agreement resulting from the use of density functional theory [52] and other more sophisticated methods.

This simple TB approach can be used to understand the optical properties of other conjugated systems of practical interest, such as cromophores used in organic light emitting devices or building blocks of biological molecules. We strongly believe that this method can be a powerful tool in teaching a variety of topics in physics of materials.

Acknowledgments. The authors acknowledge the financial support received from SNSF and UEFISCDI under the Romanian-Swiss Research Program, through the joint grant RSRP #IZERO-142144/1 and PN-II-ID-RSRP-1/2012.

REFERENCES

1. B. N. Finklestein and G. E. Horowitz, Z. Physik, **48**, 118 (1928).
2. F. Bloch, Z. Physik, **52**, 555 (1929).
3. C. Kittel, *Introduction to Solid State Physics*, 6th ed., John Wiley, New York, 1986.
4. E. Kaxiras, *Atomic and Electronic Structure of Solids*, Cambridge University Press, Cambridge, 2003.
5. J.K. Burdett, Progr. Solid State Chem., **15**, 173 (1984).
6. R. Hoffmann, *Solids and Surfaces: A chemist's view of bonding in extended structures*, Wiley-VCH, New York, 1988.
7. E. Hückel, Z. Physik **60**, 423 (1930); **70**, 204 (1931); **72**, 310 (1931); **76**, 628 (1932); **83**, 632 (1933).
8. J.P. Lowe, *Quantum Chemistry*, 2nd ed., Academic Press, New York, 1993.
9. C.J. Dalton, L.E. Friedrich, J. Chem. Educ., **52**, 721 (1975).
10. J. Farrell, J. Chem. Educ., **52**, 351 (1985).
11. G. Taubmann, J. Chem. Educ., **67**, 96 (1992).
12. D.A. Bahnick, J. Chem. Educ., **71**, 171 (1994).
13. E.F. Healy, J. Chem. Educ., **72**, A120 (1995).
14. C. Sotiriou-Leventis, S.B. Hanna, N. Leventis, J. Chem. Educ., **73**, 295 (1996).
15. B.G. Moore, J. Chem. Educ., **77**, 785 (2000).
16. J.M. LoBue, J. Chem. Educ., **79**, 1378 (2002).
17. S. Nordholm, A. Back, G.B. Bacskay, J. Chem. Educ., **84**, 1201 (2007).
18. R. Ramakrishnan, J. Chem. Educ., **90**, 132 (2013).
19. M. Buchheit and P.D. Loly, Am. J. Phys., **40**, 289 (1972).
20. C. Kuncser, A. Kuncser, G. Maftei, S. Antohe, Rom. Rep. Phys., **64**, 1119 (2012).
21. S. Moraru, I. Stoica, F.F. Popescu, Rom. Rep. Phys., **63**, 577 (2011).
22. M. Garabet, I. Neacşu, F.F. Popescu, Rom. Rep. Phys., **62**, 918 (2010).
23. C.G. Bostan, N. Dina, M. Bulgariu, S. Crăciun, M. Dafinei, C. Chițu, I. Staicu, S. Antohe, Rom. Rep. Phys., **63**, 543 (2011).
24. N. Dina, S. Crăciun, M. Bulgariu, S. Antohe, Rom. Rep. Phys., **64**, 868 (2012).
25. B. O'Regan and M. Grätzel, Nature, **353**, 737 (1991).
26. M. Grätzel, Nature, **414**, 338 (2001).
27. A. Hagfeldt, G. Boschloo, L. Sun, L. Kloo, H. Pettersson, Chem. Rev., **110**, 6595 (2010).

28. Y. Chi, P.T. Chou, Chem. Soc. Rev., **39**, 638 (2010).
29. G. Zhou, W.-Y. Wong, S. Suo, J. Photochem. Photobio C, **11**, 133 (2010).
30. A. Yella, H.W. Lee, H.N. Tsao, C. Yi, A.K. Chandiran, M.K. Nazeeruddin, E.W.G. Diau, C.Y. Yeh, S.M. Zakeeruddin, M. Grätzel, Science, **334**, 629 (2011).
31. J. Burschka, N. Pellet, S.-J. Moon, R.Humphry-Baker, P. Gao, M.K. Nazeeruddin, M. Grätzel, Nature, **499**, 316 (2013).
32. A. Mishra, M.K.R. Fischer, P. Bauerle, Angew. Chem. Int. Ed., **48**, 2474 (2009).
33. Z.S. Wang, Y. Cui, K. Hara, Y. Dan-oh, C. Kasada, A. Shinpo, Adv. Mater., **19**, 1138 (2007).
34. Y. Ooyama and Y. Harima, Eur. J. Org. Chem., 2903 (2009).
35. K. Hara, K. Sayama, Y. Ohga, A. Shinpo, S. Suga, H. Arakawa, Chem. Comm., 569 (2001).
36. K. Hara, T. Sato, R. Katoh, A. Furube, Y. Ohga, A. Shinpo, S. Suga, K. Sayama, H. Sugihara, and H. Arakawa, J. Phys. Chem. B, **107**, 597 (2003).
37. K. Hara, Z.-S. Wang, T. Sato, A. Furube, R. Katoh, A. Furube, H. Sugihara, Y. Dan-oh, C. Kasada, A. Shinpo, S. Suga, J. Phys. Chem. B, **109**, 15476 (2005).
38. Z.S. Wang, Y. Cui, Y. Dan-oh, C. Kasada, A. Shinpo, K. Hara, J. Phys. Chem. C, **111**, 7224 (2007).
39. A. Streiwieser, *Molecular Orbital Theory for Organic Chemists*, Wiley, New York, 1961, p. 135.
40. *** Mathematica, version 8.0, Wolfram Research, Inc., Champaign, Illinois, 2010.
41. *** MathCAD, version 15.0, Parametric Technology Corporation, Needham, Massachusetts, 2010.
42. *** Maple, Version 17, Maplesoft, Waterloo, Ontario, 2013.
43. *** The Supplementary Materials consist of a Mathematica notebook illustrating the calculation of the energy spectrum and the molecular orbitals of the basic coumarin.
44. L. Johansson, Ark. Fys., **31**, 201 (1966).
45. L.J. Schaad, B.A. Hess, J. Am. Chem. Soc., **94**, 3068 (1972).
46. Microsoft Corporation, Visio, version 14.0, Redmond, Washington (2010).
47. J. Roncali, Macromol. Rapid Commun., **28**, 1761 (2007).
48. S. Yang, P. Olishevski, M. Kertesz, Synth. Met., **141**, 171 (2004).
49. R. Hoffmann, J. Chem. Phys., **39**, 1397 (1963).
50. M. J. Frisch, G. W. Trucks, H. B. Schlegel, G. E. Scuseria, M. A. Rob, J. R. Cheeseman, J. A. Montgomery Jr., T. Vreven, K. N. Kudin, J. C. Burant, J. M. Millam, S. S. Iyengar, J. Tomasi, V. Barone, B. Mennucci, M. Cossi, G. Scalmani, N. Rega, G. A. Petersson, H. Nakatsuji, M. Hada, M. Ehara, K. Toyota, R. Fukuda, J. Hasegawa, M. Ishida, T. Nakajima, Y. Honda, O. Kitao, H. Nakai, M. Klene, X. Li, J. E. Knox, H. P. Hratchian, J. B. Cross, V. Bakken, C. Adamo, J. Jaramillo, R. Gomperts, R. E. Stratmann, O. Yazyev, A. J. Austin, R. Cammi, C. Pomelli, J. W. Ochterski, P. Y. Ayala, K. Morokuma, G. A. Voth, P. Salvador, J. J. Dannenberg, V. G. Zakrzewski, S. Dapprich, A. D. Daniels, M. C. Strain, O. Farkas, D. K. Malick, A. D. Rabuck, K. Raghavachari, J. B. Foresman, J. V. Ortiz, Q. Cui, A. G. Baboul, S. Clifford, J. Cioslowski, B. B. Stefanov, G. Liu, A. Liashenko, P. Piskorz, I. Komaromi, R. L. Martin, D. J. Fox, T. Keith, M. A. Al-Laham, C. Y. Peng, A. Nanayakkara, M. Challacombe, P. M. W. Gill, B. Johnson, W. Chen, M. W. Wong, C. Gonzalez, and J. A. Pople, *Gaussian 03*, Gaussian, Inc., Wallingford, Connecticut, 2003.
51. R. Dennington, T. Keith, and J. Millam, *GaussView*, Version 4, Semichem Inc., Shawnee Mission, Kansas, 2003.
52. C.I. Oprea, P. Panait, F. Cimpoesu, M. Ferbinteanu, M.A. Gîrțu, Materials, **6**, 2372 (2013).